

1-1-2022

Assessment of hole quality, thermal analysis, and chip formation during dry drilling process of gray cast iron ASTM A48

Numan Habib

Aamer Sharif

Aqib Hussain

Muhammad Aamir

Edith Cowan University, m.aamir@ecu.edu.au

Khaled Giasin

See next page for additional authors

Follow this and additional works at: <https://ro.ecu.edu.au/ecuworks2022-2026>



Part of the [Civil and Environmental Engineering Commons](#)

[10.3390/eng3030022](https://doi.org/10.3390/eng3030022)

Habib, N., Sharif, A., Hussain, A., Aamir, M., Giasin, K., & Pimenov, D. Y. (2022). Assessment of hole quality, thermal analysis, and chip formation during dry drilling process of gray cast iron ASTM A48. *Eng*, 3(3), 301-310.

<https://doi.org/10.3390/eng3030022>

This Journal Article is posted at Research Online.





<https://ro.ecu.edu.au/ecuworks2022-2026/1433>

Authors

Numan Habib, Aamer Sharif, Aqib Hussain, Muhammad Aamir, Khaled Giasin, and Danil Yurievich Pimenov

Article

Assessment of Hole Quality, Thermal Analysis, and Chip Formation during Dry Drilling Process of Gray Cast Iron ASTM A48

Numan Habib ¹, Aamer Sharif ¹ , Aqib Hussain ¹, Muhammad Aamir ² , Khaled Giasin ³ 
and Danil Yurievich Pimenov ^{4,*} 

¹ Department of Mechanical Engineering, CECOS University of Information Technology and Emerging Sciences, Peshawar 25000, Pakistan; numanhabib@cecos.edu.pk (N.H.); aamer@cecos.edu.pk (A.S.); iamaqibhussain@gmail.com (A.H.)

² School of Engineering, Edith Cowan University, Joondalup 6027, Australia; m.aamir@ecu.edu.au

³ School of Mechanical and Design Engineering, University of Portsmouth, Portsmouth PO1-3DJ, UK; khaled.giasin@port.ac.uk

⁴ Department of Automated Mechanical Engineering, South Ural State University, 454080 Chelyabinsk, Russia

* Correspondence: danil_u@rambler.ru

Abstract: The cutting parameters in drilling operations are important for high-quality holes and productivity improvement in any manufacturing industry. This study investigates the effects of spindle speed and feed rate on temperature, surface roughness, hole size, circularity, and chip formation during dry drilling of gray cast iron ASTM A48. The results showed that the temperature increased as spindle speed and feed rate increased. The surface roughness had an inverse relationship with the spindle speed and direct relation with the feed rate. Furthermore, hole size increased with increased spindle speed and decreased as the feed rate increased, while hole circularity decreased with increasing both the spindle speed and feed rate. The analysis of variance (ANOVA) indicated that the spindle speed had the highest percentage contribution of 56.24% on temperature, followed by the feed rate with 42.35%. The surface roughness was highly influenced by the feed rate and the spindle speed with 55% and 44.12%, respectively. While the hole size was highly influenced by the feed rate with a 74.18% percentage contribution, and the contribution of spindle speed was 21.36%. In addition, the feed rate has a percentage contribution of 70.82% on circularity, which is higher than the spindle speed of 24.26% percentage contribution. The results also showed that thick and discontinuous chips were generated at higher feed rates, while long continuous chips were produced at high spindle speeds.

Keywords: drilling; gray cast iron; thermal analysis; circularity; hole size; surface roughness; chips formation



Citation: Habib, N.; Sharif, A.; Hussain, A.; Aamir, M.; Giasin, K.; Pimenov, D.Y. Assessment of Hole Quality, Thermal Analysis, and Chip Formation during Dry Drilling Process of Gray Cast Iron ASTM A48. *Eng* **2022**, *3*, 301–310. <https://doi.org/10.3390/eng3030022>

Academic Editor: Manoj Khandelwal

Received: 24 April 2022

Accepted: 23 June 2022

Published: 27 June 2022

Publisher's Note: MDPI stays neutral with regard to jurisdictional claims in published maps and institutional affiliations.



Copyright: © 2022 by the authors. Licensee MDPI, Basel, Switzerland. This article is an open access article distributed under the terms and conditions of the Creative Commons Attribution (CC BY) license (<https://creativecommons.org/licenses/by/4.0/>).

1. Introduction

Gray cast iron A48 has unique mechanical properties, including low friction and wear resistance [1]. It is also used to produce automotive parts such as pistons, cylinder liners, heads, clutch plates, and brake drums because of its high damping capacity and high carbon content. Additionally, it is used to manufacture flywheels, gearboxes, pumps, valves, pipes, ingot molds, and machine-tool parts [2].

The process parameters, such as feed rate, spindle speed, cutting fluid, tool diameter, and chip formation play a key role in hole quality [3,4]. Similarly, an appropriate selection of machine setup and cutting tools during drilling operations is essential to avoid rapid tool wear and low-quality holes [5–7]. In addition, inappropriate process parameters can produce torque and undesired thermal stresses on the workpiece and cutting tool, which leads to undesirable distortion and hence reduces tool life and hole quality [8].

Literature showed various studies on the effect of process parameters to improve the quality of holes. For instance, Islam et al. [9] analyzed the influence of process variables such as depth of cut, spindle speed (n), and feed rate (f) on the material removal rate and hole quality in the turning operation of gray cast iron A48. The results showed that n has a higher impact on the material removal rate than the depth of cut and f . Selvan et al. [10] worked on abrasive water jet cutting of gray cast iron A48 to determine the influence of abrasive mass flow rate, nozzle traverse speed, and water pressure on the cutting depth during the cutting process. According to the findings of this study, these operational parameters directly affect the depth of the cut. Furthermore, a regression analysis was conducted to evolve an empirical model for measuring the depth of cut through abrasive materials. Ogedengbe et al. [11] studied the effect of numerous parameters on material removal rates for the annealed and unannealed gray cast iron under wet and dry cutting conditions. It was concluded that the best result in terms of machining is achieved with annealed and wet cutting conditions. Souza et al. [12] concluded that the heat generated in the primary shear zone was smaller than that created in the secondary shear zone in drilling gray cast iron A48. Therefore, the tool and the chip must disperse a significant amount of heat produced in the cutting zone. The result shows that temperature is significantly affected by n , which has a significant impact on the performance of the tool at higher n . Moreover, the n raises the cutting temperature by influencing strain rates in the primary and secondary shear planes. Mills [13] examined that using PCBN tools for machining gray cast iron significantly increases the n by obtaining high productivity compared to cemented carbide. However, for the machining of gray cast iron, the PCBN tool can be operated normally when the n ranges from 500 to 1500 m/min, while in some specific cases, the n may be over 2000 m/min. Guesser et al. [14] analyzed the surface roughness of the gray iron by selecting the process parameters such as R_a , R_y , and R_z at different n . The roughness value is higher at n of 400 m/min than that acquired at a higher n . De Sousa et al. [15] investigated the cutting forces of EM-245 gray cast iron in turning operating using a silicon nitride (Si_3N_4) ceramic tool. They observed that the range of cutting parameters for the formation of built-up edge is much higher than machining steels.

The above literature reveals limited research on the assessment of hole quality and thermal analysis during drilling of gray cast iron A48. Therefore, the current work is focused on the effect of various drilling parameters on thermal analysis, chip formation, and characteristics of hole quality, including surface roughness, hole size deviation, and circularity. Additionally, the impact of input parameters on temperature, surface roughness, hole size, and circularity were evaluated using ANOVA.

2. Materials and Methods

2.1. Workpiece Material

In this study, a gray cast iron ASTM A48 was selected with a length of 150 mm, a width of 50 mm, and a thickness of 13 mm. The properties of gray cast iron ASTM A48 are shown in Table 1, while Table 2 depicts its chemical composition.

Table 1. Properties of gray cast iron A48 [16].

Properties	Value
Density (g/cm^3)	7.15
Hardness (BHN)	174–210
Ultimate tensile strength (MPa)	207
Melting temperature (F)	2050–2120

Table 2. Chemical composition of gray cast iron A48 [16].

Element	Composition
Carbon	3.1–3.3
Sulfur	0.05–0.12

Table 2. *Cont.*

Element	Composition
Phosphorus	0.02–0.1
Silicon	2.1–2.3
Manganese	0.5–0.9

2.2. Machine Setup, Cutting Parameters, and Cutting Tool

The drilling operation was performed on a vertical milling machine (Model: Victoria-Elliott U2, London, UK) using the cutting parameters as given in Table 3. In addition, a Dormer high-speed steel (HSS) drill bit was used for the drilling process. The details of the drill bit are shown in Table 4. Due to environmental concerns, the experiments were conducted without coolants.

Table 3. Cutting parameters.

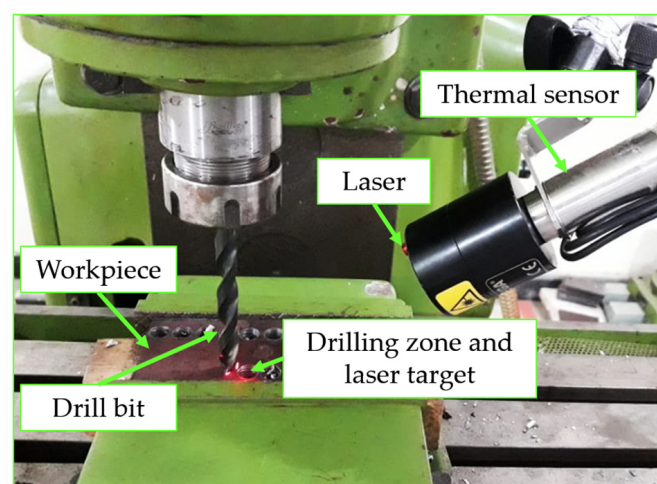
Levels	Feed Rate (m/min)	Spindle Speed (n)	Cutting Speed (V_c)
		rpm	m/min
1	0.013	43	1.35
2	0.025	77	2.42
3	0.034	141	4.43
4	0.049	308	9.67

Table 4. Details of drill bit.

Drill Bit Material	Description
Material	High-speed steel
Diameter	10 mm
Point angle	118°
Helix angle	30°

2.3. Measurement of Temperature

The temperature was measured using an infrared pyrometer sensor (Model: OS-180-USB-LSTL OMEGA, London, UK) with the same procedure used by Riaz et al. [17]. First, the pyrometer was mounted, clamped, and positioned at a point from the desired drilling hole using magnetic support. Next, the laser beam was accurately focused on the desired location to record the temperature, as shown in Figure 1.

**Figure 1.** Experimental setup.

2.4. Post-Drilling Experiments

The surface roughness parameter (R_a) was measured using a Mitutoyo (SJ-201) surface roughness tester at 0° and 90° of each hole. In addition, a coordinate measuring machine (CMM, Taichung, Taiwan) was used to measure circularity error and hole deviation from the nominal size. A ruby probe with a diameter of 2 mm circulated continually around the hole’s internal wall was used. The measuring probe’s scanning speed was adjusted at 1 mm per second, allowing 400 points to be captured while rotating around the inside circle of a hole. Moreover, a DSLR camera 5220 was used to analyze the chip formation produced during the drilling of gray cast iron A48.

2.5. Analysis of Variance

Finally, the effect of input parameters on drilling output parameters was performed using analysis of variances (ANOVA) with a 95% confidence interval similar to the previous studies [5].

3. Results and Discussions

3.1. Thermal Analysis

Microstructural changes, tolerance errors and distortions, work material adhesiveness on the tool’s cutting edges, and residual strains in the subsurface layers can all occur as a result of an excessive increase in temperature [3,18]. Figure 2 illustrates the impact of n and f feed rate on temperature during the drilling process of gray cast iron. The results show an increase in the temperature due to n and f . Therefore, the impact of n was absorbed to be more on temperature than f , as indicated in Table 5. The percentage contribution of n was 56.24%, and the f was 42.35%. Therefore, the rise in temperature during the drilling process depends on machining parameters. According to Chen [19], the higher n can generate frictional heat on the tool–workpiece interface and significantly affects the tool performance. Nouari et al. [20] also reported that the f and n increase the temperature. This is because a high n causes plastic deformation, which leads to increases in temperature. Moreover, higher f increases the contact length between the chips and tool, which leads to temperature increases. Additionally, the temperature rise increased the reduction in tool life.

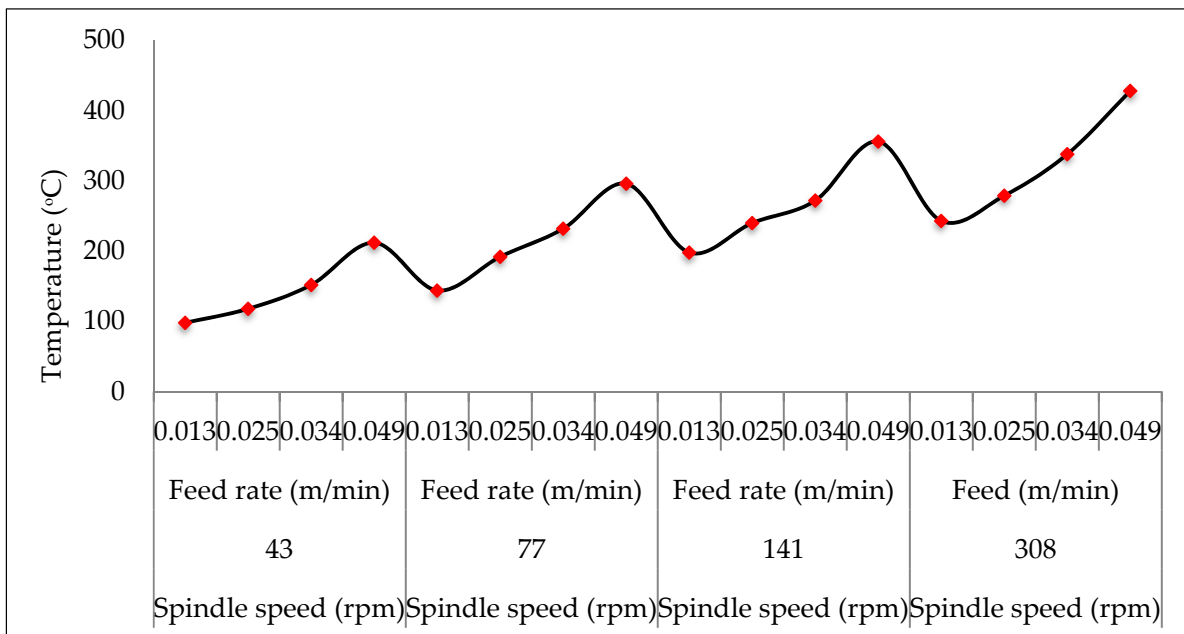


Figure 2. Temperature with different feed rates and cutting speeds.

Table 5. Analysis of variances for temperature.

Source	DF	Seq SS	Contribution	Adj S.S.	Adj MS	F-Value	p-Value
Model	6	119,206	98.59%	119,206	19,867.7	105.07	0.000
Linear	6	119,206	98.59%	119,206	19,867.7	105.07	0.000
Spindle speed	3	67,999	56.24%	67,999	22,666.3	119.87	0.000
Feed rate	3	51,207	42.35%	51,207	17,069.1	90.27	0.000
Error	9	1702	1.41%	1702	189.1	-	-
Total	15	120,908	100.00%	-	-	-	-

3.2. Assessment of Hole Quality

3.2.1. Surface Roughness

Surface roughness (Ra) refers to the irregularities caused by machining operations on the surface of a machined part [21]. It is considered vital when evaluating machining performance and significantly influences manufacturing processes and their cost [22]. This study obtained Ra under various n and f , as shown in Figure 3. The results showed that both the n and f affect the surface roughness. This agrees with the results from the thermal analysis as discussed above that higher n increases the temperature. The Ra value directly relates to f and has an inverse relation with n . The decrease in Ra value with an increasing n is explained due to the surface temperature of the workpiece. As n increases, the workpiece surface temperature rises because resistance supplied by the material against a tool decreases, which softens the material resulting in a better surface finish at high n [23]. Moreover, the built-up edge formation might have also affected the Ra [24]. Additionally, the Ra value increased with the increase in f and a likely explanation for this might be that a high thrust force needed to deform the thick layer of the chip, which induces more aggressive vibration in the tool and results in a high surface finish [25]. Furthermore, it is investigated that Ra increased when the chip thickness increased. A short, thick, and discontinuous chip increases the Ra . However, Ra decreases with long, thin and continuous chip formation [26]. The effect of f was found to be more significant than the n . This could be confirmed from ANOVA in Table 6 in which the f has a percentage contribution of 55.00% while n has an impact of 44.12% on the Ra .

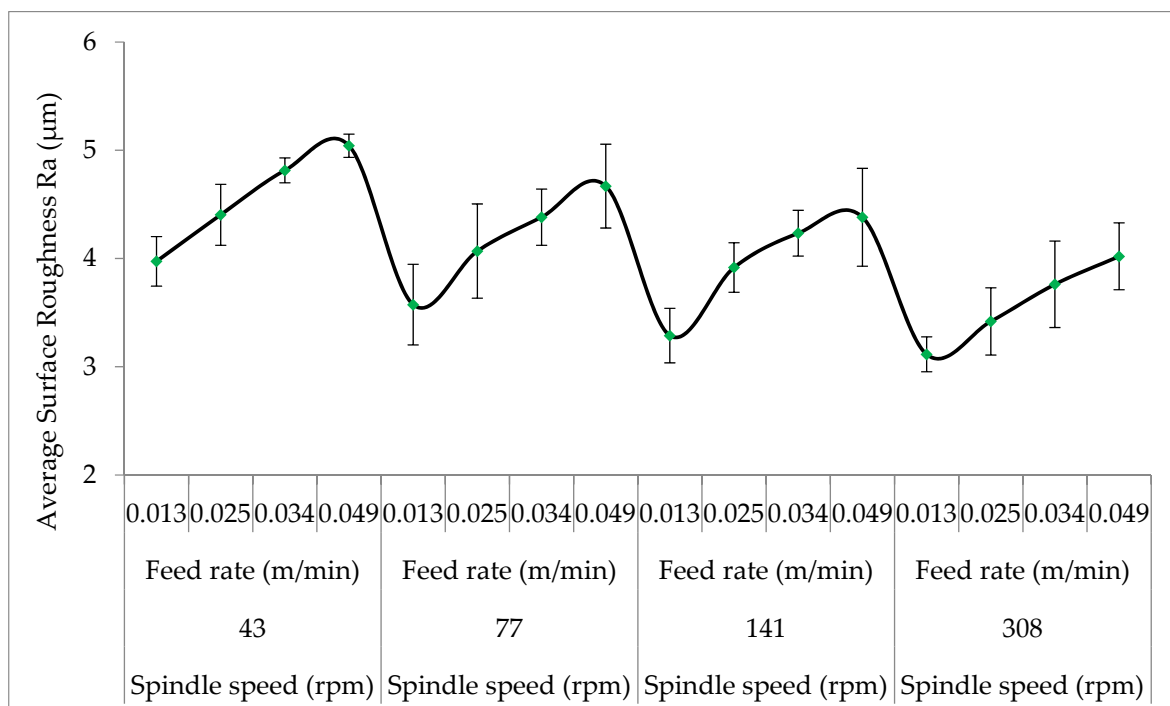


Figure 3. Average surface roughness.

Table 6. Analysis of variances for surface roughness.

Source	DF	Seq SS	Contribution	Adj SS	Adj MS	F-Value	p-Value
Model	6	4.46877	99.12%	4.46877	0.744794	168.57	0.000
Linear	6	4.46877	99.12%	4.46877	0.744794	168.57	0.000
Spindle speed	3	1.98912	44.12%	1.98912	0.663042	150.06	0.000
Feed rate	3	2.47964	55.00%	2.47964	0.826547	187.07	0.000
Error	9	0.03977	0.88%	0.03977	0.004418	-	-
Total	15	4.50853	100.00%	-	-	-	-

3.2.2. Hole Size

Any machined product performance is influenced by the nominal hole size variation, often known as diametric deviation [27]. The holes deviation from the nominal size (10 mm) under varying n and f is shown in Figure 4. Results showed the oversized holes range between 10.133 and 10.276 mm. The hole size was observed to decrease significantly with increasing f . Increasing f from 0.013 m/min to 0.049 m/min, hole size values decreased from 10.240 mm to 10.133 mm at a constant n of 43 rpm. This could be due to the chip’s high thickness at a high f , which induced the cutting process to become unsteady and caused continual jerks. Moreover, small thickness chips are produced at low f , allowing jerk-free and consistent drilling with little deviation from nominal size [28]. However, the hole size values increased from 10.240 mm to 10.276 mm with an increase in n from 43 rpm to 308 rpm at a constant f of 0.013 m/min. The increase in hole size with an increase in n is due to drilling vibration and chatter phenomena. Furthermore, at a higher n , the temperature considerably impacts drilled hole accuracy [25]. Therefore, the current study shows that dimensional accuracy improved with an increase in the f at low n . The ANOVA result from Table 7 shows that the f percentage contribution was 74.18%, while the percentage contribution of n was 21.36%.

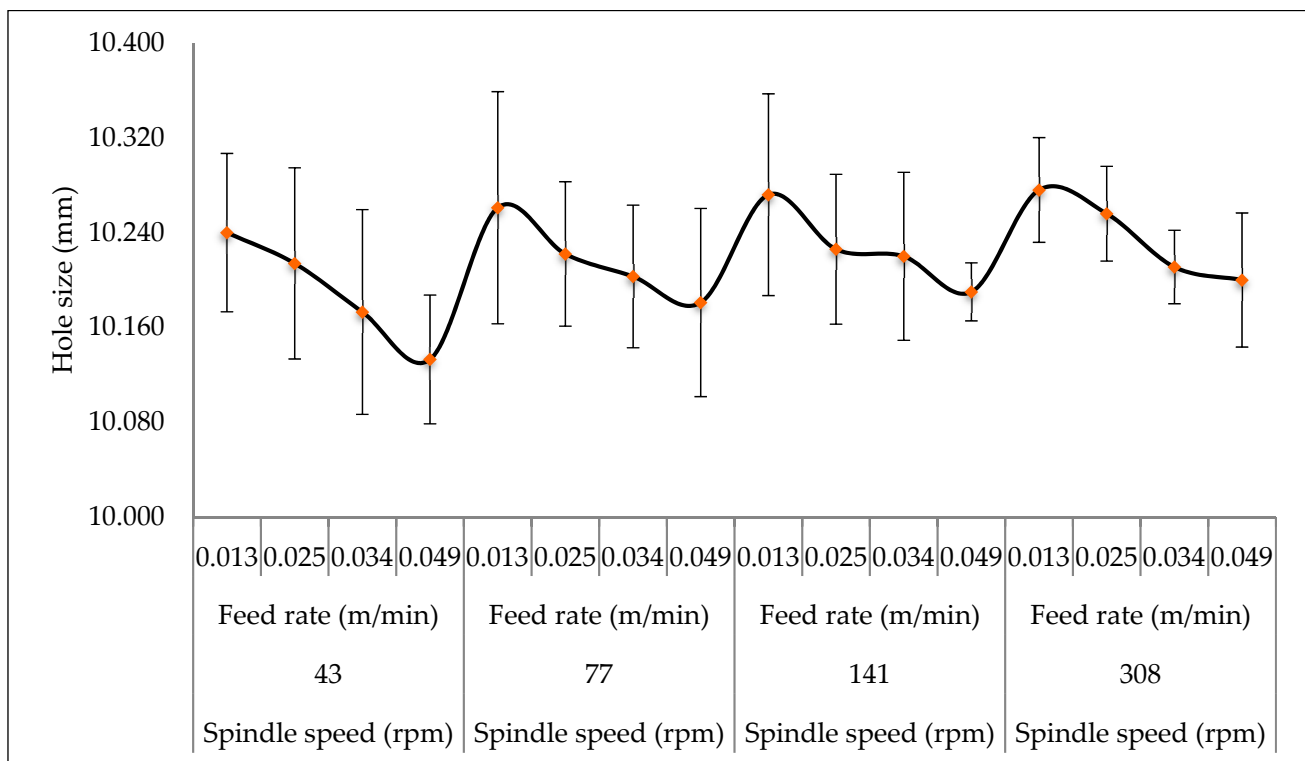


Figure 4. Average hole size.

Table 7. Analysis of variances for hole size.

Source	DF	Seq SS	Contribution	Adj SS	Adj MS	F-Value	p-Value
Model	6	0.021121	95.54%	0.021121	0.00704	64.32	0.001
Linear	6	0.021121	95.54%	0.021121	0.00704	64.32	0.001
Spindle speed	3	0.004722	21.36%	0.004722	0.001574	14.38	0.001
Feed rate	3	0.016399	74.18%	0.016399	0.005466	49.94	0.000
Error	9	0.000985	4.46%	0.000985	0.000109	-	-
Total	15	0.022105	100.00%	-	-	-	-

3.2.3. Circularity

The two-dimensional radial tolerance called circularity or roundness error indicates how close a component with a diametrical cross-section is to a true circle [7,29]. Figure 5 depicts the circularity varying f and n . In the current study, the circularity error decreased significantly with increasing both f and n . Circularity values decreased from 0.034 mm to 0.027 mm by increasing f from 0.013 m/min to 0.049 m/min at a constant n of 43 rpm. This was possibly due to the discontinuous chips obtained at a high f . However, at a low f , continuous chips tangled around the cutting tool, disturbing the dynamic balance, and inducing high vibration. Moreover, increasing n from 43 rpm to 308 rpm also decreases the circularity value from 0.034 mm to 0.031 mm at a constant feed rate of 0.013 m/min. The decrease in circularity with increasing n could be due to the low contact duration between chip and tool [30]. In the current study, the circularity or roundness error for all drilling holes is less than 0.040 mm. Moreover, from the ANOVA in Table 8, the influence of f in affecting the circularity was greater with a percentage contribution of 70.82%, while the percentage contribution of n was 24.26%.

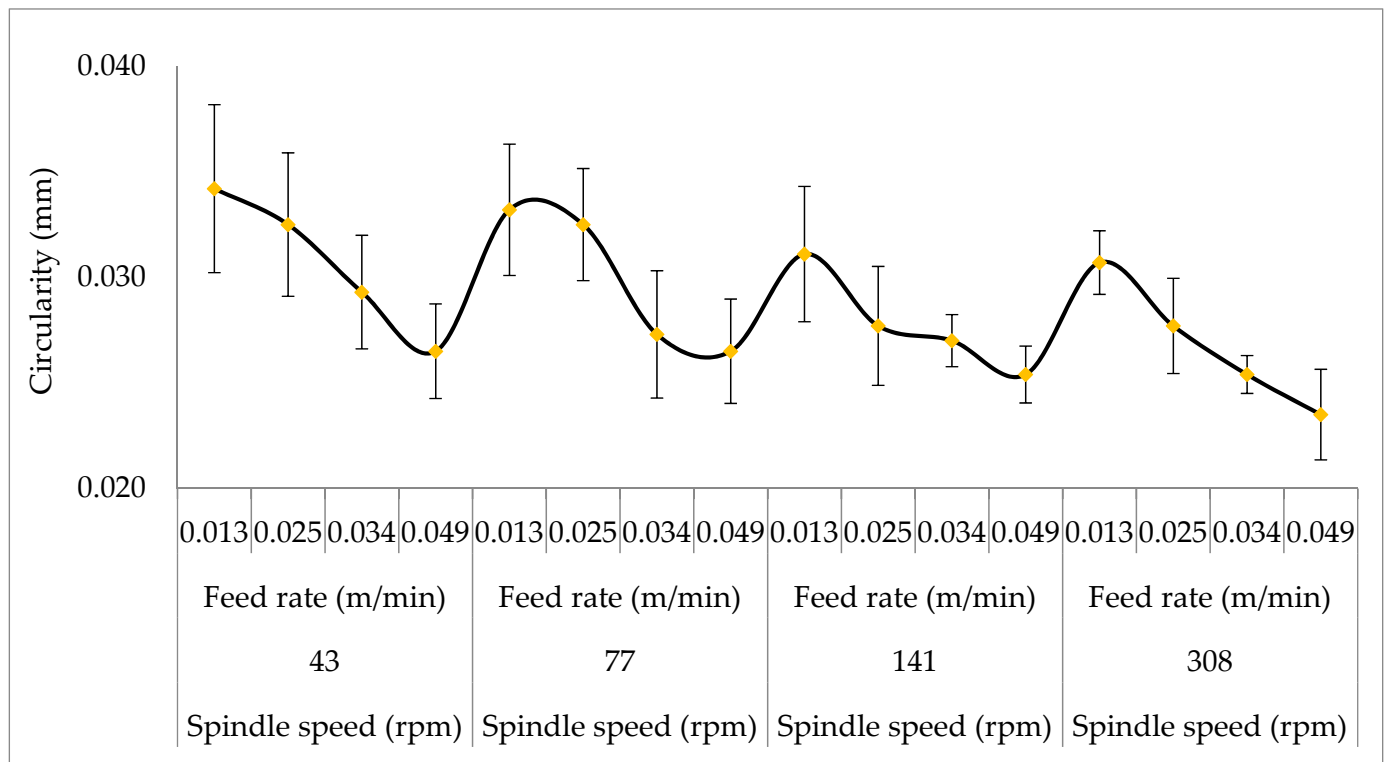


Figure 5. Average circularity.

Table 8. Analysis of variances for circularity error.

Source	DF	Circularity					
		Seq SS	Contribution	Adj SS	Adj MS	F-Value	p-Value
Model	6	0.0000148	95.08%	0.0000148	0.00005	57.79	0.001
Linear	6	0.0000148	95.08%	0.0000148	0.00005	57.79	0.001
Spindle speed	3	0.000038	24.26%	0.000038	0.000013	14.79	0.001
Feed rate	3	0.000110	70.82%	0.000110	0.000037	43.17	0.000
Error	9	0.000008	4.92%	0.000008	0.000001	-	-
Total	15	0.000155	100.00%	-	-	-	-

3.3. Chip Morphology

Figure 6 shows chips produced during dry drilling of gray cast iron A48. Based on the ISO 3685-1977 chip classification chart [31], different types of chips are developed during the machining process, such as tubular chips, spiral chips, helical chips, ribbon chips, arc chips, elemental, and needle chips. These chips are further divided into long, short, and snarled chips. This work generated connected-arc chips at n of 43 rpm and a feed rate of 0.013 m/min. However, as the n increased from 41 rpm to 308 rpm, connected-arc chips converted into long and snarled-tubular chips. Moreover, when the f increases from 0.013 m/min to 0.049 m/min and the n increases from 43 rpm to 141 rpm, the connected-arc chips are converted into short-elemental chips. Furthermore, increasing f from 0.013 m/min to 0.049 m/min at 308 rpm results in the formation of loose-arc chips.

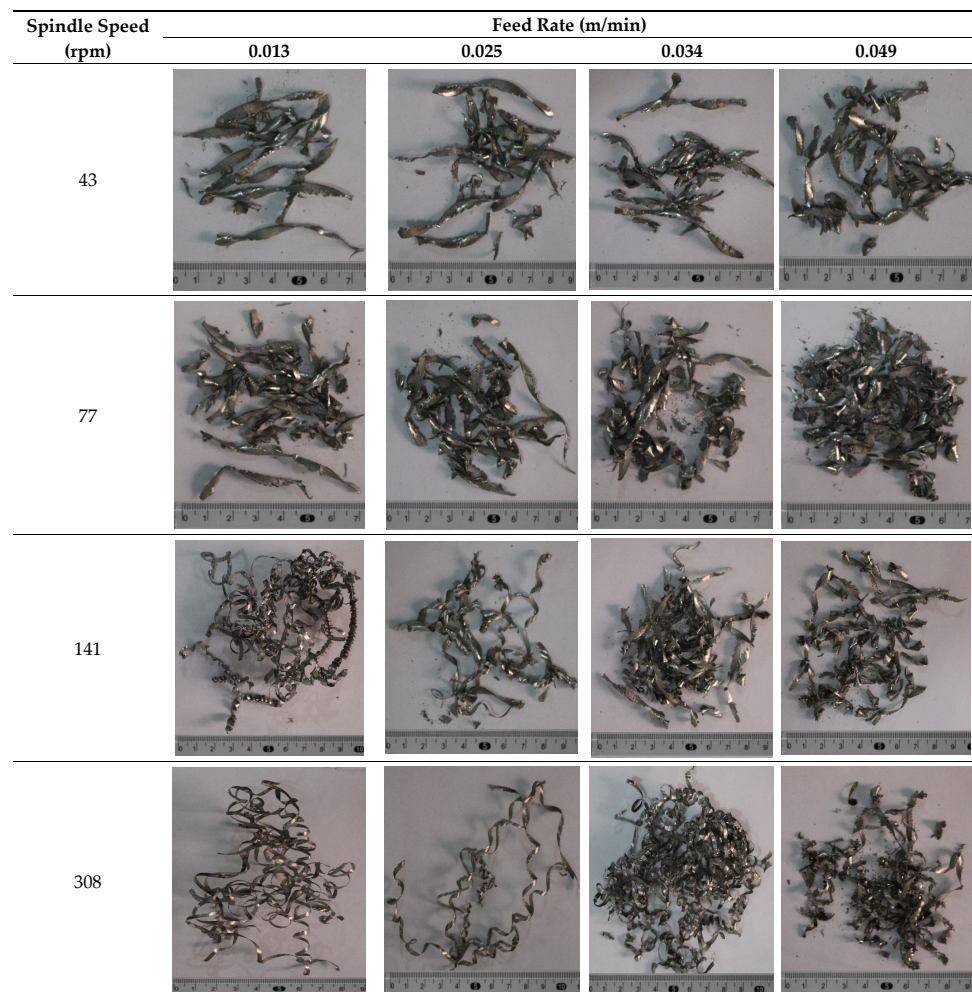


Figure 6. Formation of chips during the dry drilling process.

Figure 6 also shows that varying n influenced the length of the chips during drilling of gray cast iron A48. A high temperature caused by a high n resulted in material ductility, hence producing longer chips [32]. Further, the thickness of the chip is inversely related to n and directly related to f . The f is more influential in the current study because the cross-sectional area of the chip increased at a high f [33]. Furthermore, as n increases from 43 rpm to 308 rpm, more elongated chips are formed, and enhanced surface roughness is observed. However, an increase in f results in thick and discontinuous chips and leads to a high surface roughness of the drilled hole.

4. Conclusions

The conclusions drawn from the study are:

The temperature increased with an increase in both spindle speed and feed rate. Based on ANOVA results, the spindle speed showed the higher percentage contribution of 56.24% than the feed rate with an impact of 42.35%. The surface roughness was also affected by the spindle speed and feed rate. However, the high spindle speed decreased the surface roughness, while high surface roughness was observed at high feed rates. ANOVA results revealed that the effect of feed rate on surface roughness was 55.00% compared to the spindle speed (44.12%). The hole size had a direct relation to the spindle speed and an inverse relation with feed rate. From ANOVA results, the feed rate showed the highest percentage contribution of 74.18%, and spindle speed had a percentage contribution of 21.36%. In addition, increasing feed rate and spindle speed lowered circularity error. Similarly, the ANOVA result showed that the feed rate had the highest percentage contribution of 70.82% compared to spindle speed, with a contribution percentage of 24.26%. Additionally, increasing the feed rate from 0.013 m/min to 0.049 m/min generated thick and discontinuous chips, while long continuous chips were achieved with a high spindle speed of 308 rpm.

Author Contributions: Conceptualization, A.H., A.S., M.A. and N.H.; methodology, A.H., A.S. and N.H.; validation, M.A., K.G. and D.Y.P.; investigation, N.H., A.S. and A.H.; writing—original draft preparation, N.H., A.S. and A.H.; writing—review and editing, K.G., D.Y.P. and M.A. All authors have read and agreed to the published version of the manuscript.

Funding: This research received no external funding.

Institutional Review Board Statement: Not applicable.

Informed Consent Statement: Not applicable.

Data Availability Statement: The data presented in this study are available on request.

Acknowledgments: The authors are highly grateful for the support and facilitation at the manufacturing lab at CECOS University and Peshawar Light Engineering Centre at CECOS Industrial Liaison Centre, Industrial Estate, Peshawar, Pakistan.

Conflicts of Interest: The authors declare no conflict of interest.

References

1. Riahi, A.; Alpas, A. Wear map for grey cast iron. *Wear* **2003**, *255*, 401–409. [[CrossRef](#)]
2. Upadhyay, S.; Saxena, K.K. Effect of Cu and Mo addition on mechanical properties and microstructure of grey cast iron: An overview. *Mater. Today Proc.* **2020**, *26*, 2462–2470. [[CrossRef](#)]
3. Aamir, M.; Giasin, K.; Tolouei-Rad, M.; Vafadar, A. A review: Drilling performance and hole quality of aluminium alloys for aerospace applications. *J. Mater. Res. Technol.* **2020**, *9*, 12484–12500. [[CrossRef](#)]
4. Aamir, M.; Giasin, K.; Tolouei-Rad, M.; Ud Din, I.; Hanif, M.I.; Kuklu, U.; Pimenov, D.Y.; Ikhlaq, M. Effect of Cutting Parameters and Tool Geometry on the Performance Analysis of One-Shot Drilling Process of AA2024-T3. *Metals* **2021**, *11*, 854. [[CrossRef](#)]
5. Aamir, M.; Tolouei-Rad, M.; Giasin, K.; Vafadar, A. Feasibility of tool configuration and the effect of tool material, and tool geometry in multi-hole simultaneous drilling of Al2024. *Int. J. Adv. Manuf. Technol.* **2020**, *111*, 861–879. [[CrossRef](#)]
6. Aamir, M.; Tolouei-Rad, M.; Giasin, K. Multi-spindle drilling of Al2024 alloy and the effect of TiAlN and TiSiN-coated carbide drills for productivity improvement. *Int. J. Adv. Manuf. Technol.* **2021**, *114*, 3047–3056. [[CrossRef](#)]

7. Aamir, M.; Davis, A.; Keeble, W.; Koklu, U.; Giasin, K.; Vafadar, A.; Tolouei-Rad, M. The Effect of TiN-, TiCN-, TiAlN-, and TiSiN Coated Tools on the Surface Defects and Geometric Tolerances of Holes in Multi-Spindle Drilling of Al2024 Alloy. *Metals* **2021**, *11*, 1103. [CrossRef]
8. Nomani, J.; Pramanik, A.; Hilditch, T.; Littlefair, G. Machinability study of first generation duplex (2205), second generation duplex (2507) and austenite stainless steel during drilling process. *Wear* **2013**, *304*, 20–28. [CrossRef]
9. Islam, M.M.; Hossain, S.S.; Bhuyan, M.S.A. Optimization of metal removal rate for ASTM A48 grey cast iron in turning operation using Taguchi method. *Int. J. Mater. Sci. Eng.* **2015**, *3*, 134–146. [CrossRef]
10. Selvan, M.C.P.; Raju, N.M.S.; Rajavel, R. Effects of process parameters on depth of cut in abrasive waterjet cutting of cast iron. *Int. J. Sci. Eng. Res.* **2011**, *2*, 1–5.
11. Ogedengbe, T.S.; Yezeed, O.; Yussouf, A.A. Effect of Annealing on Machinability of Grey Cast Iron. *Int. J. Eng. Res. Technol.* **2018**, *2*, 4090–4994.
12. Souza, J.; Nono, M.; Ribeiro, M.; Machado, J.; Silva, O. Cutting forces in turning of gray cast iron using silicon nitride based cutting tool. *Mater. Des.* **2009**, *30*, 2715–2720. [CrossRef]
13. Mills, B. Recent developments in cutting tool materials. *J. Mater. Proc. Technol.* **1996**, *56*, 16–23. [CrossRef]
14. Guesser, W.L.; Pereira, F.S.; Boehs, L. Surface changes during turning of grey cast iron. *Int. J. Mach. Mach. Mater.* **2016**, *18*, 313–324. [CrossRef]
15. De Sousa, J.A.G.; Sales, W.F.; Machado, A.R. A review on the machining of cast irons. *Int. J. Adv. Manuf. Technol.* **2018**, *94*, 4073–4092. [CrossRef]
16. Gray Iron ASTM A48. Available online: <https://www.pentictionfoundry.com/news/gray-iron-astm-a48-class-30/> (accessed on 14 March 2022).
17. Riaz, A.A.; Hussain, G.; Ullah, N.; Wei, H.; Alkahtani, M.; Khan, M.N. An investigation on the effects of tool rotational speed and material temper on post-ISF tensile properties of Al2219 alloy. *J. Mater. Res. Technol.* **2021**, *10*, 853–867. [CrossRef]
18. Kishawy, H.; Dumitrescu, M.; Ng, E.-G.; Elbestawi, M. Effect of coolant strategy on tool performance, chip morphology and surface quality during high-speed machining of A356 aluminum alloy. *Int. J. Mach. Tools Manuf.* **2005**, *45*, 219–227. [CrossRef]
19. Chen, W. Cutting forces and surface finish when machining medium hardness steel using CBN tools. *Int. J. Mach. Tools Manuf.* **2000**, *40*, 455–466. [CrossRef]
20. Nouari, M.; List, G.; Girot, F.; Coupard, D. Experimental analysis and optimisation of tool wear in dry machining of aluminium alloys. *Wear* **2003**, *255*, 1359–1368. [CrossRef]
21. Al-Tameemi, H.A.; Al-Dulaimi, T.; Awe, M.O.; Sharma, S.; Pimenov, D.Y.; Koklu, U.; Giasin, K. Evaluation of cutting-tool coating on the surface roughness and hole dimensional tolerances during drilling of al6061-t651 alloy. *Materials* **2021**, *14*, 1783. [CrossRef]
22. Aamir, M.; Tolouei-Rad, M.; Giasin, K.; Nosrati, A. Recent advances in drilling of carbon fiber-reinforced polymers for aerospace applications: A review. *Int. J. Adv. Manuf. Technol.* **2019**, *105*, 2289–2308. [CrossRef]
23. Dwivedi, S.; Kumar, S.; Kumar, A. Effect of turning parameters on surface roughness of A356/5% SiC composite produced by electromagnetic stir casting. *J. Mech. Sci. Technol.* **2012**, *26*, 3973–3979. [CrossRef]
24. Barani, A.; Amini, S.; Paktinat, H.; Fadaei Tehrani, A. Built-up edge investigation in vibration drilling of Al2024-T6. *Ultrasonics* **2014**, *54*, 1300–1310. [CrossRef] [PubMed]
25. Kurt, M.; Kaynak, Y.; Bagci, E. Evaluation of drilled hole quality in Al 2024 alloy. *Int. J. Adv. Manuf. Technol.* **2008**, *37*, 1051–1060. [CrossRef]
26. Ngermtong, S.; Butdee, S. Surface roughness prediction with chip morphology using fuzzy logic on milling machine. *Mater. Today Proc.* **2020**, *26*, 2357–2362. [CrossRef]
27. Aamir, M.; Tolouei-Rad, M.; Giasin, K.; Vafadar, A.; Koklu, U.; Keeble, W. Evaluation of the Surface Defects and Dimensional Tolerances in Multi-Hole Drilling of AA5083, AA6061, and AA2024. *Appl. Sci.* **2021**, *11*, 4285. [CrossRef]
28. Uddin, M.; Basak, A.; Pramanik, A.; Singh, S.; Krolczyk, G.M.; Prakash, C. Evaluating hole quality in drilling of Al 6061 alloys. *Materials* **2018**, *11*, 2443. [CrossRef]
29. Koklu, U.; Morkavuk, S.; Featherston, C.; Haddad, M.; Sanders, D.; Aamir, M.; Pimenov, D.Y.; Giasin, K. The effect of cryogenic machining of S2 glass fibre composite on the hole form and dimensional tolerances. *Int. J. Adv. Manuf. Technol.* **2021**, *115*, 125–140. [CrossRef]
30. Giasin, K.; Hodzic, A.; Phadnis, V.; Ayvar-Soberanis, S. Assessment of cutting forces and hole quality in drilling Al2024 aluminium alloy: Experimental and finite element study. *Int. J. Adv. Manuf. Technol.* **2016**, *87*, 2041–2061. [CrossRef]
31. ISO 3685:1977; Tool-life testing with single-point turning tools. International Organization for Standardization: Geneva, Switzerland, 1977.
32. Sun, J.; Guo, Y. A new multi-view approach to characterize 3D chip morphology and properties in end milling titanium Ti-6Al-4V. *Int. J. Mach. Tools Manuf.* **2008**, *48*, 1486–1494. [CrossRef]
33. Zhu, Z.; Guo, K.; Sun, J.; Li, J.; Liu, Y.; Chen, L.; Zheng, Y. Evolution of 3D chip morphology and phase transformation in dry drilling Ti6Al4V alloys. *J. Manuf. Process.* **2018**, *34*, 531–539. [CrossRef]